Critical properties of short-range Ising spin glasses on a Wheatstone-bridge hierarchical lattice

Sebastião T. O. Almeida[1,2,*] and Fernando D. Nobre[1,3,†]

[1]*Centro Brasileiro de Pesquisas Físicas, Rua Xavier Sigaud 150, 22290-180 Rio de Janeiro RJ, Brazil*

[2]*Colégio Técnico da Universidade Federal Rural do Rio de Janeiro, Seropédica, 23891-000 Rio de Janeiro RJ, Brazil*

[3]*National Institute of Science and Technology for Complex Systems, Rua Xavier Sigaud 150, 22290-180 Rio de Janeiro RJ, Brazil*

(Received 21 May 2015; published 3 August 2015)

An Ising spin-glass model with nearest-neighbor interactions, following a symmetric probability distribution, is investigated on a hierarchical lattice of the Wheatstone-bridge family characterized by a fractal dimension $D \approx 3.58$. The interaction distribution considered is a stretched exponential, which has been shown recently to be very close to the fixed-point coupling distribution, and such a model has been considered lately as a good approach for Ising spin glasses on a cubic lattice. An exact recursion procedure is implemented for calculating site magnetizations, $m_i = \langle S_i \rangle_T$, as well as correlations between pairs of nearest-neighbor spins, $\langle S_i S_j \rangle_T$ ($\langle\,\rangle_T$ denote thermal averages), for a given set of interaction couplings on this lattice. From these local magnetizations and correlations, one can compute important physical quantities, such as the Edwards-Anderson order parameter, the internal energy, and the specific heat. Considering extrapolations to the thermodynamic limit for the order parameter, such as a finite-size scaling approach, it is possible to obtain directly the critical temperature and critical exponents. The transition between the spin-glass and paramagnetic phases is analyzed, and the associated critical exponents β and ν are estimated as $\beta = 0.82(5)$ and $\nu = 2.50(4)$, which are in good agreement with the most recent results from extensive numerical simulations on a cubic lattice. Since these critical exponents were obtained from a fixed-point distribution, they are universal, i.e., valid for any coupling distribution considered.

DOI: 10.1103/PhysRevE.92.022102 PACS number(s): 05.70.Jk, 75.10.Nr, 64.60.F−, 64.60.De

I. INTRODUCTION

The renormalization group (RG) represents one of the most successful approximations for studying critical phenomena [1,2]. In the case of a real-space RG, its application for Bravais lattices usually leads to the generation of additional terms in the Hamiltonian after each RG step, in such a way that one is obliged to impose truncations that may affect directly the results. One way to overcome this difficulty concerns the introduction of hierarchical lattices (HLs) [2,3] as approaches to Bravais lattices, which present the notable advantage that the real-space RG becomes exact for pure systems defined on the former. This occurs essentially due to the fact that the HLs are constructed in the inverse order of the application of the RG procedure, through successive similar operations at each hierarchical level, e.g., at each level one replaces bonds by unit cells, as shown in Fig. 1. In this case, the approximation is concerned with the particular choice of the appropriate HL to emulate the Bravais lattice under study. Since a given Bravais lattice may be approached by different HLs, in this choice one has to take into account both the accuracy of the results and the difficulty in dealing with the particular HL used.

Although the RG cannot be considered in general as an exact procedure for random systems on HLs, it is expected to represent a good approximation, since in many cases pure systems appear as particular limits of random models. A random magnetic model that has been the object of attention of much research throughout recent decades is the Ising spin glass (SG) [4–9]. Its simple formulation in terms of binary variables has attracted many researchers, who have followed several computational and analytical procedures, leading to a wide variety of results and interpretations, some of them contradictory, so that the model remains very controversial.

The HLs have been very useful in the study of Ising SGs [10–27], mostly due to the possibility of obtaining estimates, which are in some cases very close to those of more time-consuming techniques, by performing relatively low-time-consuming numerical computations. Some results related to critical-temperature estimates, as well as those concerning the lower critical dimension d_l, above which one finds a SG phase at finite temperatures, are worth mentioning. (i) The SG critical temperatures on the Migdal-Kadanoff (MK) lattice [28,29] of fractal dimension $D = 3$, for symmetric Gaussian and bimodal distributions [10], present relative discrepancies of about 7% when compared with the recent estimates from Monte Carlo simulations on a cubic lattice [30]. (ii) Recently, the estimates of item (i) were improved further through the hierarchical lattices defined by the cell of Fig. 1(b) [25], which, when compared with the estimates of Ref. [30], yields a relative discrepancy of about 3% in the Gaussian case, whereas for the symmetric bimodal distribution the two estimates essentially coincide (leading to a relative discrepancy of about 0.3%). (iii) The bounds for the lower critical dimension, $2 < d_l < 3$, were first obtained on MK lattices [10], a few years before their confirmation in Refs. [11,31–34] through studies of excitations from ground states; these domain-wall analyses were improved later [35,36], reinforcing the early conclusions. (iv) A recent combination of extensive numerical and theoretical results on Bravais lattices [37] suggested the lower critical dimension to be exactly $d_l = 5/2$, confirming the early estimate of Ref. [12] for MK lattices. (v) Studies on a self-dual hierarchical lattice

*Author to whom all correspondence should be addressed: stalme@cbpf.br

†fdnobre@cbpf.br

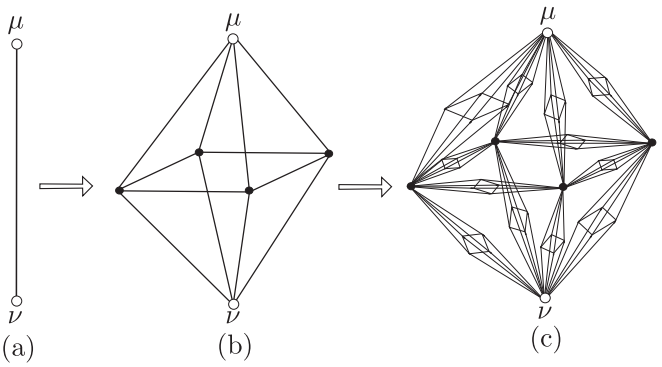

FIG. 1. Two first steps in the generation of the Wheatstone-bridge hierarchical lattice investigated herein, which has been used in the literature to approach the cubic lattice [3]. In each step, one replaces a bond (a) by the unit cell shown in (b) (characterized by a fractal dimension $D \approx 3.58$), where the empty circles (μ and ν) represent external sites of the cell, whereas the black circles are internal sites to be decimated in the RG procedure. The same procedure carried in (b) leads to (c).

with scaling factor $b = 3$ and fractal dimension $D = 2$ led to an estimate for the stiffness exponent y [14] ($y = -1/\nu$, where ν is the exponent associated with the divergence of the correlation length at zero temperature) in agreement with those obtained from other, more time-consuming, numerical approaches on a square lattice. An analysis of the $\pm J$ Ising SG model [22] on the same hierarchical lattice gave a ferromagnetic-paramagnetic critical frontier that represents a good approximation for that of the corresponding model on a square lattice.

A significant effort has been made on the nearest-neighbor-interaction Ising SG model on a cubic lattice, for which it is generally accepted nowadays that a SG phase occurs at finite temperatures [8–12,27,30,38–43]; it should be emphasized that some of these works have required extensive computational efforts. Motivated by the good agreement between the critical-temperature estimates obtained in Ref. [25], for the Ising SG model with nearest-neighbor interactions defined on the HL constructed through the procedure shown in Fig. 1, when compared with those obtained in Ref. [30] by means of extensive numerical simulations, herein we study further critical properties of this model on the HL of Fig. 1. In the next section, we define the model and the numerical procedure to be used, emphasizing an exact recursion method for calculating the local magnetizations of all sites of this lattice. Since we deal with symmetric probability distributions for the couplings, only two phases will appear, namely the paramagnetic (**P**) and spin-glass (**SG**) phases; herein we focus on the critical behavior associated with the **P**-**SG** transition. In Sec. III we make use of the site magnetizations in order to compute the Edwards-Anderson order parameter and other important physical quantities. Particularly, considering a finite-size scaling, we compute the critical exponents β and ν associated with the **P**-**SG** transition; the good agreement with estimates obtained for the cubic lattice from different numerical methods is discussed. Finally, in Sec. IV we present our conclusions.

II. THE MODEL AND THE RECURSION PROCEDURE

Herein we investigate the Ising SG on the HL constructed through the procedure shown in Fig. 1, defined by the Hamiltonian

$$\mathcal{H} = -\sum_{\langle ij \rangle} J_{ij} S_i S_j \qquad (S_i = \pm 1). \tag{1}$$

The sum $\sum_{\langle ij \rangle}$ applies to pairs of nearest-neighbor spins of the HL, whereas the $\{J_{ij}\}$ represent independent random couplings acting on each pair of spins of the lattice. For the purpose of the present work, the couplings $\{J_{ij}\}$ may be considered initially as following any symmetric distribution, characterized by finite moments, e.g., Gaussian, bimodal, and uniform distributions; however, for computational reasons, we will use a distribution very close to the fixed-point distribution, as will be explained next.

As usual in the RG procedure, after each decimation step the set of coupling constants $\{J_{ij}\}$, as well as the temperature T, vary in such a way that the probability distribution $P(K_{ij})$, associated with the dimensionless ratios $\{K_{ij}\}$ [$K_{ij} = J_{ij}/(kT)$], changes its shape. Precisely at the phase **P**-**SG** transition, one starts with a given probability distribution $P(K_{ij})$, and after a few RG iterations one reaches the fixed-point distribution $P^*(K_{ij})$, which will not change in further RG steps. Strictly speaking, in order to approach such a distribution, one needs to be exactly at the critical temperature T_c, associated with this transition. Operationally, for a given initial distribution, the associated critical temperature is estimated approximately, by following numerically $P(K_{ij})$, within the standard narrowing RG procedure (see, e.g., Refs. [10,24,25]). Hence, starting with different initial distributions will take some steps of the RG procedure to approach $P^*(K_{ij})$, and after this, all initial distributions considered will behave in a similar way, so that critical properties should be computed with $P^*(K_{ij})$. As a direct consequence, critical exponents are universal, i.e., independent of the initial distribution considered [18].

Flux diagrams representing the evolution of two probability distributions $P(K_{ij})$ under RG iterations, constructed from a Gaussian (with unit variance) and the stretched exponential

$$P(J_{ij}) = \frac{\exp(-|J_{ij}/J|^{\delta})}{2J\Gamma\left(1+\frac{1}{\delta}\right)}, \tag{2}$$

with $J = 1.22(3)$ and $\delta = 1.60(2)$ are shown in Fig. 2. These diagrams are represented in suitable variables [12,18], so that throughout the evolution of the distributions one has the following: (i) The unstable fixed-point, associated with the phase transition **P**-**SG** and assigned to the fixed-point distribution $P^*(K_{ij})$ (indicated by a blue arrow). (ii) The two attractors characterizing the corresponding phases are given by $[\tanh^2 K_{ij}]_P \to 0$ and $1/[K_{ij}^2]_P^{1/2} \to \infty$ (**P** attractor), as well as $[\tanh^2 K_{ij}]_P \to 1$ and $1/[K_{ij}^2]_P^{1/2} \to 0$ (**SG** attractor). (iii) These attractors define two basins of attraction, such that for initial distributions corresponding to values of $[\tanh^2 K_{ij}]_P$ above (below) those of the fixed-point distribution, one is driven to the **SG** (**P**) attractor. (iv) From the two initial distributions considered, one sees that the stretched exponential of Eq. (2) corresponds essentially to the fixed-point distribution, whereas the Gaussian presents a "larger distance"

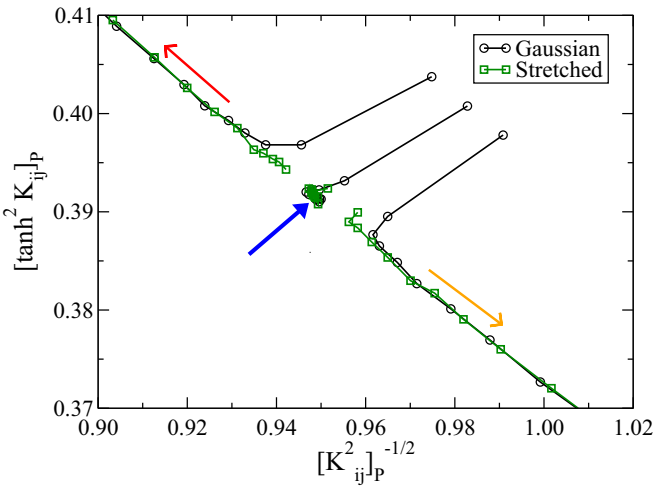

FIG. 2. (Color online) Flux diagrams of two probability distributions $P(K_{ij})$ are represented in suitable variables [12,18]. These distributions were constructed, respectively, from a Gaussian (with unit variance) and the stretched exponential of Eq. (2), for the coupling distributions of the Ising SG model of Eq. (1), on the HL defined according to Fig. 1. For each of these two distributions, three different temperatures were considered, namely $T > T_c$ (fluxes toward increasing abscissas), $T < T_c$ (fluxes toward decreasing abscissas), and $T = T_c$. For the critical temperature associated with each distribution, we have used the estimates of Ref. [44], namely $(kT_c/J) = 0.9821$ (Gaussian distribution) and $(kT_c/J) = 0.948$ (stretched-exponential distribution). The blue arrow indicates the point associated with the fixed-point distribution $P^*(K_{ij})$, from which one concludes that the distribution of Eq. (2) may be considered as a good approximation of the fixed-point distribution, whereas the Gaussian distribution presents a "larger distance" from $P^*(K_{ij})$. In the variables used, $[\,]_P$ represent averages over the corresponding probability distributions.

with respect to the fixed-point distribution. (v) In the variables used, the abscissa is related to the renormalized dimensionless temperature at each step of the RG process, so that the critical temperature associated with the fixed-point distribution is given by $(kT_c^{\rm FD}/J) \equiv [(K_{ij}^*)^2]_P^{-1/2}$, to be computed for $P(K_{ij}) = P^*(K_{ij})$. Recently, a thorough analysis was carried out showing that the distribution of Eq. (2) is indeed very close to the fixed-point distribution associated with the **P-SG** phase transition [44]. In this work, it is also shown that different initial distributions, when considered at their corresponding critical temperatures T_c, approach such a unique (i.e., universal) fixed-point distribution after some RG steps.

A procedure for calculating the site magnetizations exactly was developed for the Ising ferromagnet on HLs of the MK family in Ref. [45]; later on, this method was implemented for random Ising systems, such as Ising SGs [16] and the random-field Ising model [46], on the same HLs. Herein, such a procedure is extended for Ising SGs on the lattice defined in Fig. 1, as explained next. First of all, the whole HL is generated up to a hierarchy level of order N, where all sites and bonds should be labeled appropriately. Then, all bonds generated at level N are assigned to coupling constants $\{J_{ij}\}$, drawn from a given probability distribution. The standard RG is followed $N-1$ times, taking care to store each renormalized coupling in each hierarchy level, until one reaches the coupling of order zero [Fig. 1(a)]. Then, one follows the inverse process, the so-called aggregation process, defining arbitrarily the initial magnetizations at the external sites μ and ν of Fig. 1(a), from which all site magnetizations will be calculated (to be described below), considering the values of the couplings assigned to each bond, already stored in the RG process. It is important to mention that the number of couplings and sites increases very rapidly, at each step of the generation process of the present HL, so that the procedure requires a high computational cost; as an example, in the present case, the seventh hierarchy ($N = 7$) was the largest size studied, with $12^7 = 35\,831\,808$ couplings and 13 029 750 sites. If one starts with initial distributions for the couplings very different from the fixed-point distribution $P^*(K_{ij})$, one needs to discard iterations corresponding to the highest hierarchy levels, which contain the large majority of the couplings (11/12 of the couplings belong to the last generation). Consequently, for the sake of computational cost, it becomes crucial that the initial distribution should be very close to $P^*(K_{ij})$.

Hence, we start the RG procedure with all bonds generated at hierarchy level N assigned to coupling constants $\{J_{ij}\}$, drawn from the probability distribution of Eq. (2), so as to follow the usual decimation of the internal sites of a unit cell [cf. Fig. 1(b)], leading to renormalized quantities associated with the external sites. The corresponding RG equations may be written in the general form [24,25]

$$K'_{\mu\nu} = \frac{1}{4}\ln\left(\frac{\mathcal{Z}_{--}\,\mathcal{Z}_{++}}{\mathcal{Z}_{-+}\,\mathcal{Z}_{+-}}\right), \tag{3}$$

where $\mathcal{Z}_{S_\mu S_\nu}$ represent partition functions associated with the Hamiltonian $\mathcal{H}$ for a given unit cell with the external spins kept fixed ($S_\mu, S_\nu = \pm 1$),

$$\mathcal{Z}_{S_\mu S_\nu} = {\rm Tr}_{\{S_i\,(i\neq\mu,\nu)\}}\,[\exp(-\beta\mathcal{H})]. \tag{4}$$

It should be mentioned that the recursion relation of Eq. (3) is used in the present approach for computing the flux diagram of Fig. 2, the fixed-point probability distribution, as well as the critical temperature associated with the **P-SG** phase transition.

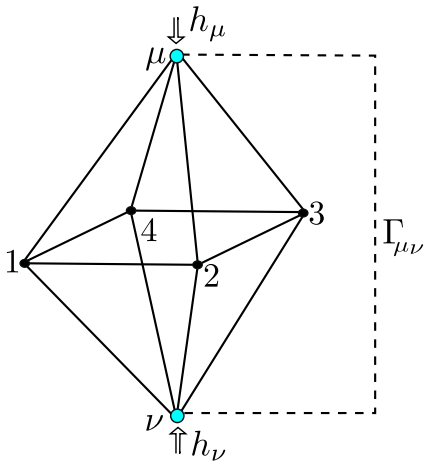

FIG. 3. (Color online) Basic unit cell showing the labeled internal sites to be used in the calculations, with μ and ν denoting the external sites; $\Gamma_{\mu\nu}$, h_μ, and h_ν represent, respectively, effective coupling and fields acting upon the external spins of the basic cell.

Now we describe how one can calculate local magnetizations and correlations functions exactly on the HL considered; this method is analogous to the one developed for random Ising systems on HLs of the MK family, explained in detail in Refs. [16,46]. The essential idea is illustrated in Fig. 3 and is based on the fact that the partition function of the whole HL at its hierarchy level N may be expressed in terms of quantities defined for a single unit cell, containing both internal and external contributions of the cell. Particularly, the effective interaction $\Gamma_{\mu\nu}$ between the external spins and the effective fields h_μ and h_ν acting on these spins are unknown quantities, which carry the contributions of the rest of the HL acting upon the basic cell, to be determined recursively. These effective quantities arise when we perform the trace over the spin variables of the remaining lattice by considering the equivalence of the partition function of the Hamiltonian for hierarchy level N and the one for the basic unit cell of Fig. 3, with effective fields acting on the spins of its root sites, in addition to an effective coupling between these spins.

Hence, the Hamiltonian of the whole HL may be written as

$$\begin{aligned}\mathcal{H}' =& -\Gamma_{\mu\nu}S_\mu S_\nu - h_\mu S_\mu - h_\nu S_\nu - J_{12}S_1S_2 - J_{23}S_2S_3 - J_{34}S_3S_4 - J_{41}S_4S_1 \\ & - \sum_{j=1}^{4}(J_{\mu j}S_\mu S_j + J_{j\nu}S_jS_\nu) = -\Gamma_{\mu\nu}S_\mu S_\nu - h_\mu S_\mu - h_\nu S_\nu + \mathcal{H}, \end{aligned} \tag{5}$$

where the internal spins were labeled according to Fig. 3, and $\mathcal{H}$ corresponds to the internal Hamiltonian of the basic unit cell. The associated partition function is given by

$$\begin{aligned} Z =& \,\mathrm{Tr}_{(\{S_i\},S_\mu,S_\nu)}\exp\left(-\beta\mathcal{H}'\right) \\ =& \,\mathrm{Tr}_{(S_\mu,S_\nu)}\exp[\beta(\Gamma_{\mu\nu}S_\mu S_\nu + h_\mu S_\mu + h_\nu S_\nu)]\mathrm{Tr}_{(\{S_i\})} \\ & \times \exp\left\{\beta\left[J_{12}S_1S_2 + J_{23}S_2S_3 + J_{34}S_3S_4 + J_{41}S_4S_1 + \sum_{j=1}^{4}(J_{\mu j}S_\mu S_j + J_{j\nu}S_jS_\nu)\right]\right\}, \end{aligned} \tag{6}$$

and performing the trace over all spins variables, one obtains

$$Z = \mathbf{A}(e^{\mathcal{X}} + e^{\mathcal{Y}}) + \mathbf{B}(e^{\mathcal{V}} + e^{\mathcal{W}}), \tag{7}$$

where $\mathbf{A} = \sum_{i=1}^{16}\exp(R_i)$ and $\mathbf{B} = \sum_{i=17}^{32}\exp(R_i)$. The quantities R_i $(i = 1,\ldots,32)$ depend only on the couplings $\{K_{ij}\}$, presenting expressions of the type

$$R_1 = K_{23} + K_{34} - K_{12} - K_{41} - K_{\mu 2} - K_{2\nu} - K_{\mu 3} - K_{3\nu} - K_{\mu 4} - K_{4\nu} + K_{1\nu} + K_{\mu 1}, \tag{8}$$

with other $\{R_i\}$ differing from the expression above through distinct combinations of $+$ and $-$ signs; moreover, the arguments of the exponentials of Eq. (7) are given by

$$\mathcal{X} = \beta(\Gamma_{\mu\nu} - h_\mu - h_\nu), \tag{9}$$

$$\mathcal{Y} = \beta(\Gamma_{\mu\nu} + h_\mu + h_\nu), \tag{10}$$

$$\mathcal{V} = \beta(h_\mu - \Gamma_{\mu\nu} - h_\nu), \tag{11}$$

$$\mathcal{W} = \beta(h_\nu - \Gamma_{\mu\nu} - h_\mu). \tag{12}$$

The local magnetizations and pair-correlation functions associated with the spins of Fig. 3 may be calculated in the standard way,

$$\begin{aligned}\langle S_\mu\rangle =& \,Z^{-1}\mathrm{Tr}[S_\mu\exp(-\beta\mathcal{H})] \\ =& \,Z^{-1}[\mathbf{A}(-e^{\mathcal{X}} + e^{\mathcal{Y}}) + \mathbf{B}(e^{\mathcal{V}} - e^{\mathcal{W}})], \end{aligned} \tag{13}$$

$$\langle S_\nu\rangle = Z^{-1}[\mathbf{A}(-e^{\mathcal{X}} + e^{\mathcal{Y}}) + \mathbf{B}(-e^{\mathcal{V}} + e^{\mathcal{W}})], \tag{14}$$

$$\langle S_\mu S_\nu\rangle = Z^{-1}[\mathbf{A}(e^{\mathcal{X}} + e^{\mathcal{Y}}) - \mathbf{B}(e^{\mathcal{V}} + e^{\mathcal{W}})], \tag{15}$$

$$\langle S_i\rangle = Z^{-1}[\Upsilon_i(e^{\mathcal{X}} - e^{\mathcal{Y}}) + \Lambda_i(e^{\mathcal{V}} - e^{\mathcal{W}})] \quad (i = 1,2,3,4), \tag{16}$$

$$\langle S_iS_\mu\rangle = Z^{-1}[-\Upsilon_i(e^{\mathcal{X}} + e^{\mathcal{Y}}) + \Lambda_i(e^{\mathcal{V}} + e^{\mathcal{W}})] \quad (i = 1,2,3,4), \tag{17}$$

$$\langle S_i S_v\rangle = Z^{-1}[-\Upsilon_i(e^{\mathcal{X}}+e^{\mathcal{Y}})-\Lambda_i(e^{\mathcal{V}}+e^{\mathcal{W}})] \quad (i=1,2,3,4), \tag{18}$$

$$\langle S_i S_{i+1}\rangle = Z^{-1}[\Upsilon_{4+i}(e^{\mathcal{X}}+e^{\mathcal{Y}})+\Lambda_{4+i}(e^{\mathcal{V}}+e^{\mathcal{W}})] \quad (i=1,2,3), \tag{19}$$

$$\langle S_i S_{i-3}\rangle = Z^{-1}[\Upsilon_{4+i}(e^{\mathcal{X}}+e^{\mathcal{Y}})+\Lambda_{4+i}(e^{\mathcal{V}}+e^{\mathcal{W}})] \quad (i=4), \tag{20}$$

$$\langle S_i S_{i+2}\rangle = Z^{-1}[\Upsilon_{8+i}(e^{\mathcal{X}}+e^{\mathcal{Y}})+\Lambda_{8+i}(e^{\mathcal{V}}+e^{\mathcal{W}})] \quad (i=1,2), \tag{21}$$

where $\langle\,\rangle$ denote thermal averages. The quantities Υ_i and Λ_i $(i=1,\ldots,10)$ are also expressed in terms of exponentials of $\{R_i\}$ (like **A** and **B**), i.e., they depend only on the couplings $\{K_{ij}\}$, presenting lengthy expressions, e.g.,

$$\Upsilon_1 = -e^{R_1}+e^{R_2}-e^{R_3}+e^{R_4}-e^{R_5}-e^{R_6}+e^{R_7}+e^{R_8}-e^{R_9}+e^{R_{10}}-e^{R_{11}}+e^{R_{12}}-e^{R_{13}}-e^{R_{14}}+e^{R_{15}}+e^{R_{16}}, \tag{22}$$

$$\Lambda_1 = e^{R_{17}}-e^{R_{18}}-e^{R_{19}}+e^{R_{20}}+e^{R_{21}}-e^{R_{22}}+e^{R_{23}}-e^{R_{24}}+e^{R_{25}}-e^{R_{26}}+e^{R_{27}}-e^{R_{28}}+e^{R_{29}}-e^{R_{30}}-e^{R_{31}}+e^{R_{32}}, \tag{23}$$

with other $\{\Upsilon_i\}$ and $\{\Lambda_i\}$ differing from the expressions above through distinct combinations of $+$ and $-$ signs. The equations above may be manipulated to yield

$$\langle S_i\rangle = -\frac{1}{2}\left(\frac{\Upsilon_i}{\mathbf{A}}+\frac{\Lambda_i}{\mathbf{B}}\right)\langle S_\mu\rangle - \frac{1}{2}\left(\frac{\Upsilon_i}{\mathbf{A}}-\frac{\Lambda_i}{\mathbf{B}}\right)\langle S_\nu\rangle \quad (i=1,2,3,4), \tag{24}$$

$$\langle S_i S_\mu\rangle = -\frac{1}{2}\left(\frac{\Upsilon_i}{\mathbf{A}}+\frac{\Lambda_i}{\mathbf{B}}\right)\langle S_\mu S_\nu\rangle - \frac{1}{2}\left(\frac{\Upsilon_i}{\mathbf{A}}-\frac{\Lambda_i}{\mathbf{B}}\right) \quad (i=1,2,3,4), \tag{25}$$

$$\langle S_i S_\nu\rangle = -\frac{1}{2}\left(\frac{\Upsilon_i}{\mathbf{A}}-\frac{\Lambda_i}{\mathbf{B}}\right)\langle S_\mu S_\nu\rangle - \frac{1}{2}\left(\frac{\Upsilon_i}{\mathbf{A}}+\frac{\Lambda_i}{\mathbf{B}}\right) \quad (i=1,2,3,4), \tag{26}$$

$$\langle S_i S_{i+1}\rangle = \frac{1}{2}\left(\frac{\Upsilon_{4+i}}{\mathbf{A}}-\frac{\Lambda_{4+i}}{\mathbf{B}}\right)\langle S_\mu S_\nu\rangle + \frac{1}{2}\left(\frac{\Upsilon_{4+i}}{\mathbf{A}}+\frac{\Lambda_{4+i}}{\mathbf{B}}\right) \quad (i=1,2,3), \tag{27}$$

$$\langle S_i S_{i-3}\rangle = \frac{1}{2}\left(\frac{\Upsilon_{4+i}}{\mathbf{A}}-\frac{\Lambda_{4+i}}{\mathbf{B}}\right)\langle S_\mu S_\nu\rangle + \frac{1}{2}\left(\frac{\Upsilon_{4+i}}{\mathbf{A}}+\frac{\Lambda_{4+i}}{\mathbf{B}}\right) \quad (i=4), \tag{28}$$

$$\langle S_i S_{i+2}\rangle = \frac{1}{2}\left(\frac{\Upsilon_{8+i}}{\mathbf{A}}-\frac{\Lambda_{8+i}}{\mathbf{B}}\right)\langle S_\mu S_\nu\rangle + \frac{1}{2}\left(\frac{\Upsilon_{8+i}}{\mathbf{A}}+\frac{\Lambda_{8+i}}{\mathbf{B}}\right) \quad (i=1,2). \tag{29}$$

One should notice that Eqs. (24)–(29) express local magnetizations and two-spin correlation functions for the internal spins of an arbitrary unit cell in terms of the magnetizations $\langle S_\mu\rangle$ and $\langle S_\nu\rangle$, as well as the correlation function $\langle S_\mu S_\nu\rangle$, associated with the external sites of the cell. In this way, by mapping appropriately all unit cells and sites of the whole HL, one can obtain all site magnetizations, as well as the correlation functions defined above, using the recursion relations of Eqs. (24)–(29). Hence, by fixing values for $\langle S_\mu\rangle$, $\langle S_\nu\rangle$, and $\langle S_\mu S_\nu\rangle$, at hierarchy level zero, one obtains the quantities on the left-hand side of Eqs. (24)–(29) for any hierarchy level. Herein, we have used $|\langle S_\mu\rangle| = |\langle S_\nu\rangle| = |\langle S_\mu S_\nu\rangle| = 1$ at hierarchy level zero, although we have verified that for sufficiently large hierarchy levels (typically $N \geqslant 4$), these boundary conditions become irrelevant, i.e., other choices yielded similar results.

From the expressions above, one can compute important physical quantities, such as the Edwards-Anderson (EA) order parameter,

$$q_{\rm EA} = \frac{1}{N_s}\sum_i [\langle S_i\rangle^2]_J, \tag{30}$$

and the internal energy per spin,

$$u = -\frac{1}{N_b}\left[\sum_{\langle ij\rangle} J_{ij}\langle S_i S_j\rangle\right]_J, \tag{31}$$

where N_s and N_b denote, respectively, the total number of sites and bonds of the HL, whereas $[\,]_J$ represent sample averages over different configurations of the couplings $\{J_{ij}\}$. The results obtained from these quantities are presented and discussed in the next section.

III. RESULTS

Near the critical point, the EA order parameter of Eq. (30) is expected to behave like

$$q_{\rm EA} \sim |\epsilon|^\beta \quad (\epsilon = T/T_c - 1), \tag{32}$$

where β represents the standard critical exponent associated with the order parameter [4–7], and T_c is the SG critical temperature. For sufficiently large sizes, close to T_c, one expects also the scaling form,

$$q_{\rm EA} \approx L^{-\beta/\nu}\,\widetilde{q}_{\rm EA}(\epsilon L^{1/\nu}), \tag{33}$$

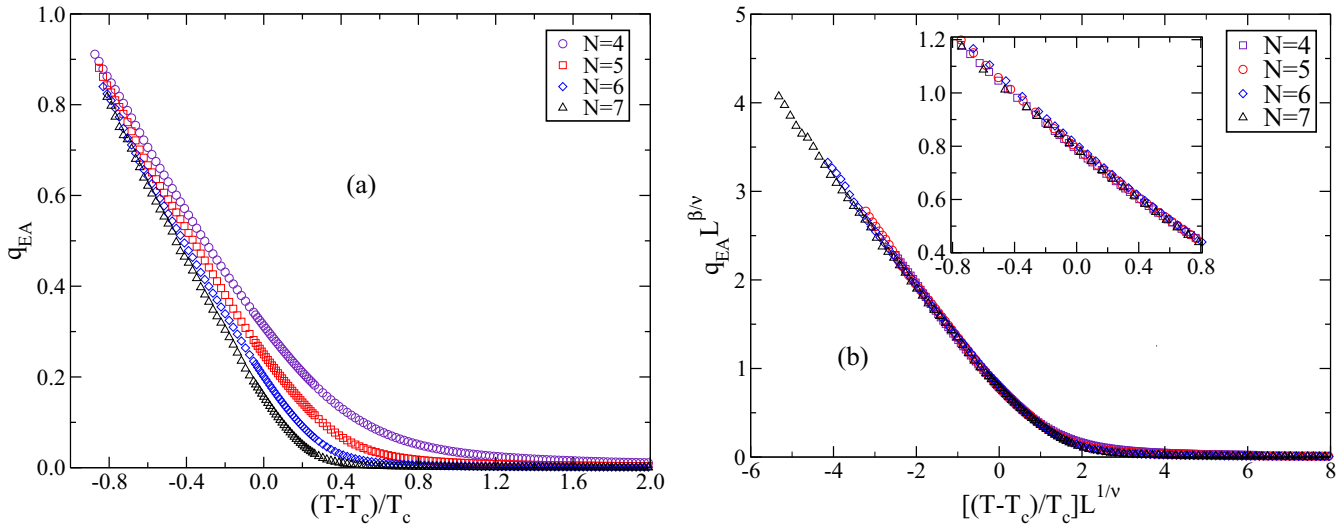

FIG. 4. (Color online) Data of the Edwards-Anderson order parameter [cf. Eq. (30)] for the Ising SG on a Wheatstone-bridge HL with $D \approx 3.58$ with different hierarchy levels N. (a) The order parameter $q_{\rm EA}$ is represented vs $(T - T_c)/T_c$; (b) a data collapse is exhibited, from which the best-collapse values for the critical exponents β and ν, as well as of the critical temperature T_c, are obtained; the inset shows an enlargement of the critical region.

where $L = 2^N$ for this HL, and $\widetilde{q}_{\rm EA}(x)$ represents a scaling function that approaches a constant when $x \to 0$.

In Fig. 4 we exhibit data for $q_{\rm EA}$ of HLs with increasing hierarchy levels N ($4 \leqslant N \leqslant 7$); it should be mentioned that the highest hierarchy level considered was $N = 7$, corresponding to a HL with $N_s = 13\,029\,750$ and $N_b = 12^7 = 35\,831\,808$. For each hierarchy level N, averages over 400 independent realizations of the disorder were performed, considering the stretched exponential of Eq. (2) as the initial distribution for the couplings. In Fig. 4(a), $q_{\rm EA}$ is represented versus $(T - T_c)/T_c$, showing the well-known finite-size effects. In Fig. 4(b), a good data collapse is obtained for both the critical region (see inset) and also out of criticality; in order to compute the critical temperature and exponents, we used an algorithm that performs an automatic search for the best-fitting values of the corresponding finite-size-scaling data [47], leading to

$$\nu = 2.50(4), \qquad \beta = 0.82(4), \qquad \frac{kT_c}{J} = 0.95(2). \tag{34}$$

The results obtained herein agree well with numerical simulations carried out for Ising SGs on the cubic lattice; indeed, the critical temperature above coincides with $(kT_c/J) = 0.951(9)$ (Gaussian distribution) [30], within the error bars. Moreover, with regard to the exponent ν, recent Monte Carlo simulations on the cubic lattice, considering different probability distributions for the couplings, yielded essentially a universal value, $\nu \approx 2.5$ [30,41–43]. In fact, considering the error bars, our estimate coincides with the most recent result from extensive numerical simulations, $\nu = 2.562(42)$ (bimodal distribution) [43]. To our knowledge, the critical exponent β has not been estimated directly in recent simulations on the cubic lattice; however, using standard scaling relations for the results of Refs. [30,41–43], we verified that typically $\beta \approx 0.78$, which coincides with our estimate (within the error bars), computed for the probability distribution of Eq. (2) that was considered herein as the fixed distribution. The agreement of our results on the tridimensional Wheatstone-bridge HL with those obtained from numerical simulations on the cubic lattice is quite impressive, which reinforces the argument that this HL represents a good approximation of a cubic lattice. However, it should be mentioned that recent estimates of the exponent ν on the same HL, calculated by considering the usual RG linearization procedure, yielded $\nu = 3.25(66)$ [48] and $\nu = 3.04(9)$ [44], which present large discrepancies with respect to the value of Eq. (34). We consider the present estimate to be more reliable, obtained by means of a direct calculation of the SG order parameter of Eq. (30), using the site magnetizations $\{\langle S_i \rangle\}$ computed exactly for the whole HL through the method described above. It is possible that these significant discrepancies may be associated with the linearization procedure used in Refs. [44,48] to obtain ν; as argued in Ref. [49], such a truncation may lead to expressive errors for SG systems.

Now, in order to calculate additional critical exponents from the estimates of Eq. (34), one has to make use of standard scaling relations, as well as of the hyperscaling relation, $2 - \alpha = \mathcal{D}\nu$. It should be mentioned that for HLs, the dimension $\mathcal{D}$ to be used in this relation is far from a trivial subject; this question has been addressed for pure systems (mostly for the Ising and q-state Potts ferromagnets on MK lattices) by several authors (see, e.g., Refs. [3,50–55]), who argued that one should use the fractal dimension D in such a relation. Since there is no similar analysis for SG systems, herein we have calculated these exponents by using both the fractal dimension $\mathcal{D} = D \approx 3.58$ as well as the spatial dimension $\mathcal{D} = d$ of the unit cell of Fig. 1(b). In fact, the total number of sites N_s that appears in Eq. (30) is given by [3,50]

$$N_s = \frac{b^{d-1}\{[(d-1)b^{d-2}(b-1)^2 + b^d]^N - 1\}}{(d-1)b^{d-2}(b-1) + (1+b+b^2)} + 2 \tag{35}$$

for a given hierarchy level N, whereas $b = 2$ and $d = 3$ for the present HL. The resulting exponents are presented in Table I,

TABLE I. Critical exponents calculated in the present work for the Ising SG on the tridimensional Wheatstone-bridge HL, considering the probability distribution of Eq. (2) as the fixed-point distribution, are compared to results from other works. The exponents β and ν were estimated from the data collapse of the EA order parameter (see Fig. 4), whereas η, γ, and α were obtained from scaling and hyperscaling relations. In the hyperscaling relation $2-\alpha = \mathcal{D}\nu$, we used both the fractal dimension of the HL, $\mathcal{D} = D = 3.58$, as well as its spatial dimension $\mathcal{D} = d = 3$ for comparison. The estimates of Ref. [18] were obtained by applying the present method to a $D = 3$ MK hierarchical lattice, whereas those of Refs. [30,42,43] resulted from numerical simulations on a cubic lattice.

	ν	β	η	γ	α
Present work ($\mathcal{D} = 3.58$)	2.50(4)	0.82(4)	−0.93(7)	7.32(13)	−6.96(4)
Present work ($\mathcal{D} = 3$)	2.50(4)	0.82(4)	−0.34(7)	5.86(25)	−5.50(4)
MK ($D = 3$) [18]	1.8(1)	0.63(3)			
Cubic lattice [30]	2.44(9)		−0.37(5)		
Cubic lattice [42]	2.45(15)	0.77(5)	−0.375(10)	5.8	−5.4(5)
Cubic lattice [43]	2.562(42)	0.782(10)	−0.3900(36)	6.13(11)	−5.69

and since the estimates of Eq. (34) are in very good agreement with those obtained from numerical simulations of Ising SGs on the cubic lattice, the results for γ, η, and α considering $\mathcal{D} = d = 3$ yield a better agreement with those of Refs. [30,41–43]. In Table I we present our results, together with those of Refs. [30,42,43], obtained from numerical simulations on a cubic lattice, as well as those of Ref. [18], computed by applying the present method to a $D = 3$ MK HL. One notices that the tridimensional Wheatstone-bridge HL leads to critical-exponent estimates that are much closer to those of the cubic lattice, when compared with the previous ones for the $D = 3$ MK HL.

The present method also allows the calculation of quantities that depend on nearest-neighbor-spin correlations $\langle S_i S_j \rangle$, like the internal energy of Eq. (31). Through use of a numerical derivation of the curve of the internal energy (see the inset of Fig. 5) with respect to the temperature, one may obtain the specific heat per spin, $c = du/dT$. In Fig. 5 we present c versus temperature, calculated from the internal energy at hierarchy level $N = 7$. Due to numerical difficulties at low temperatures, we did not succeed in computing the specific heat appropriately for $(kT/J) < 0.2$; the dashed line is a guide to the eye, showing the expected approach to zero temperature. The specific heat of Fig. 5 exhibits the standard smooth rounded maximum around the critical region, characteristic of a negative exponent α, in agreement with experimental verifications [4,5].

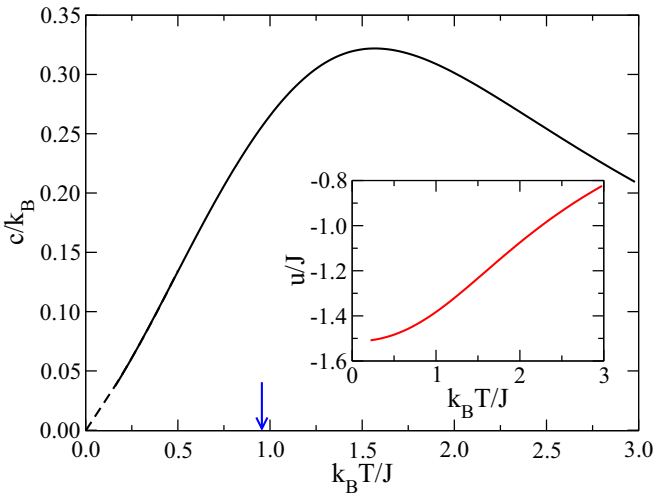

FIG. 5. (Color online) The specific heat per spin, calculated from a numerical differentiation of the internal energy of Eq. (31) with respect to the temperature, at hierarchy level $N = 7$, is exhibited in dimensionless variables. The dashed line is a guide to the eye, showing the expected tendency to zero temperature; the blue arrow indicates the critical temperature of Eq. (34). In the inset, we present the corresponding internal energy per spin in the temperature range in which the specific heat was computed.

On the other hand, the SG susceptibility defined as [4,5]

$$\chi_{\mathrm{SG}} = \frac{1}{N_s}\sum_{ij}[(\langle S_i S_j\rangle - \langle S_i\rangle\langle S_j\rangle)^2]_J \tag{36}$$

requires the computation of correlations among all possible pairs of spins of the HL, and it cannot be calculated within the present method. The equation above may be expressed as

$$\chi_{\mathrm{SG}} = \Gamma^{(1)}_{\mathrm{SG}} + \Gamma^{(2)}_{\mathrm{SG}} + \cdots, \tag{37}$$

$$\Gamma^{(1)}_{\mathrm{SG}} = \frac{1}{N_s}\sum_{\langle ij\rangle}[(\langle S_i S_j\rangle - \langle S_i\rangle\langle S_j\rangle)^2]_J, \tag{38}$$

$$\Gamma^{(2)}_{\mathrm{SG}} = \frac{1}{N_s}\sum_{\langle\langle ij\rangle\rangle}[(\langle S_i S_j\rangle - \langle S_i\rangle\langle S_j\rangle)^2]_J, \tag{39}$$

where $\Gamma^{(1)}_{\mathrm{SG}}$ carries the contribution to χ_{SG} from the nearest-neighbor pairs of spins of the HL, $\Gamma^{(2)}_{\mathrm{SG}}$ does the same for second nearest-neighbor pairs of spins, and so on. Hence, within the present method one can compute $\Gamma^{(1)}_{\mathrm{SG}}$, representing the sum of all nonlinear correlations due to nearest-neighbor pairs of spins; it is important to stress that we can compute $\Gamma^{(2)}_{\mathrm{SG}}$ only partially, considering second-nearest-neighbor pairs of spins inside a given unit cell [cf. Eqs. (24)–(29)]. In Fig. 6 we present $\Gamma^{(1)}_{\mathrm{SG}}$ versus $(T - T_c)/T_c$ for different hierarchy levels, showing an increase with the size of the system, as expected. One notices that out of criticality this quantity presents the usual behavior of χ_{SG} with temperature [4,5], although close to T_c, where correlations among all pairs of spins become important, $\Gamma^{(1)}_{\mathrm{SG}}$ does not indicate the expected divergence of $\chi_{\mathrm{SG}} \sim (|T - T_c|/T_c)^{-\gamma}$, with the exponent γ given in Table I. However, for a given L it shows a maximum

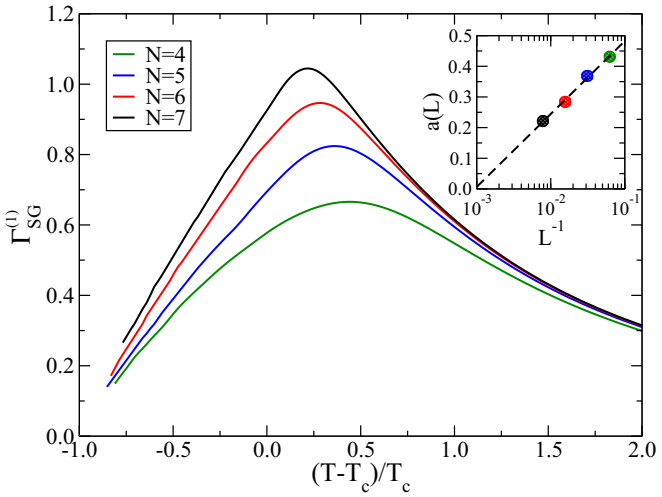

FIG. 6. (Color online) The dimensionless quantity $\Gamma^{(1)}_{SG}$, defined in Eqs. (37) and (38), is exhibited vs $(T - T_c)/T_c$ for different hierarchy levels. In the inset, we present the dimensionless distance of the maximum of each curve from the critical temperature of Eq. (34), $a(L) = [\tilde{T}(L) - T_c]/T_c$ vs L^{-1} ($L = 2^N$); the dashed line is a guide to the eye. Within our numerical accuracy, $\tilde{T}(L)$ should coincide with T_c for a hierarchy level around $N = 10$.

at a temperature $\tilde{T}(L)$, which becomes more pronounced for increasing hierarchy levels N; moreover, the inset suggests that the position of $\tilde{T}(L)$ converges to the correct critical temperature of Eq. (34), i.e., $\tilde{T}(L) \to T_c$, for increasing L. Within the numerical accuracy of Eq. (34), $\tilde{T}(L)$ should coincide with T_c for a hierarchy level around $N = 10$.

IV. CONCLUSIONS

Nearest-neighbor interaction Ising spin-glass models, defined on a hierarchical lattice of the Wheatstone-bridge family characterized by a fractal dimension $D \approx 3.58$, have been shown recently to represent a good approach for Ising spin glasses on a cubic lattice. Herein we have worked out a method for calculating exactly site magnetizations and correlations between pairs of nearest-neighbor spins for spin models defined on this hierarchical lattice. Such a procedure was introduced previously for the Ising ferromagnet [45] and spin glasses [16], defined on hierarchical lattices of the Migdal-Kadanoff family, and it has been extended for the above-mentioned hierarchical lattice of the Wheatstone-bridge family in the present work.

The method was achieved by determining exact recursion relations involving site magnetizations, $m_i = \langle S_i \rangle$, as well as nearest-neighbor correlations, $\langle S_i S_j \rangle$ ($\langle\,\rangle$ denote thermal averages), on this lattice. From these, one can compute averages over the coupling constants $[..]_J$, leading to important quantities such as $\sum_i [\langle S_i \rangle^2]_J$ and $[\sum_{\langle ij \rangle} J_{ij} \langle S_i S_j \rangle]_J$, directly related to the Edwards-Anderson order parameter and the internal energy, respectively. Considering extrapolations to the thermodynamic limit for the order parameter, such as a finite-size scaling procedure, we have obtained directly the critical temperature and critical exponents β and ν, associated with the transition between the spin-glass and paramagnetic phases. Using a symmetric stretched exponential as the fixed-point distribution for the couplings, we have estimated $\beta = 0.82(5)$ and $\nu = 2.50(4)$, which are in good agreement with the most recent results from extensive numerical simulations on a cubic lattice. These estimates represent a substantial improvement with respect to previous ones, obtained on a Migdal-Kadanoff hierarchical lattice of fractal dimension $D = 3$ [18].

Furthermore, we have also computed the specific heat, which exhibited the standard smooth rounded maximum around the critical region, in agreement with experimental verifications. The present results give further support that nearest-neighbor interaction Ising spin-glass models, defined on a hierarchical lattice of the Wheatstone-bridge family characterized by a fractal dimension $D \approx 3.58$, represent a good approach for such models on a cubic lattice.

ACKNOWLEDGMENTS

We gratefully acknowledge fruitful conversations with E. M. F. Curado; the partial financial support from CNPq and FAPERJ (Brazilian agencies) is acknowledged.

[1] J. Cardy, *Scaling and Renormalization in Statistical Physics* (Cambridge University Press, Cambridge, 1996).
[2] R. J. Creswick, H. A. Farach, and C. P. Poole, Jr., *Introduction to Renormalization Group Methods in Physics* (Wiley, New York, 1992).
[3] C. Tsallis and A. C. N. de Magalhães, Pure and random potts-like models: Real-space renormalization-group approach, Phys. Rep. **268**, 305 (1996).
[4] K. Binder and A. P. Young, Spin glasses: Experimental facts, theoretical concepts, and open questions, Rev. Mod. Phys. **58**, 801 (1986).
[5] K. H. Fischer and J. A. Hertz, *Spin Glasses* (Cambridge University Press, Cambridge, 1991).
[6] V. Dotsenko, *Introduction to the Replica Theory of Disordered Statistical Systems* (Cambridge University Press, Cambridge, 2001).
[7] H. Nishimori, *Statistical Physics of Spin Glasses and Information Processing* (Oxford University Press, Oxford, 2001).
[8] T. Castellani and A. Cavagna, Spin-glass theory for pedestrians, J. Stat. Mech. (2005) P05012.
[9] G. Parisi, Spin glasses and fragile glasses: Statics, dynamics, and complexity, Proc. Natl. Acad. Sci. (USA) **103**, 7948 (2006).
[10] B. W. Southern and A. P. Young, Real space rescaling study of spin glass behavior in three dimensions, J. Phys. C **10**, 2179 (1977).
[11] A. J. Bray and M. A. Moore, in *Heidelberg Colloquium on Glassy Dynamics*, edited by J. L. van Hemmen and I. Morgenstern, Lecture Notes in Physics Vol. 275 (Springer-Verlag, Berlin, 1987), p. 121.
[12] E. M. F. Curado and J. L. Meunier, Spin-glass in low dimensions and the Migdal-Kadanoff approximation, Physica A **149**, 164 (1988).

[13] M. Nifle and H. J. Hilhorst, New critical-point exponent and new scaling laws for short-range ising spin glasses, Phys. Rev. Lett. **68**, 2992 (1992).
[14] F. D. Nobre, Real-space renormalization-group approaches for two-dimensional Gaussian ising spin glass, Phys. Lett. A **250**, 163 (1998).
[15] M. A. Moore, H. Bokil, and B. Drossel, Evidence for the droplet picture of spin glasses, Phys. Rev. Lett. **81**, 4252 (1998).
[16] E. Nogueira, Jr., S. Coutinho, F. D. Nobre, E. M. F. Curado, and J. R. L. de Almeida, Short-range ising spin glass: Multifractal properties, Phys. Rev. E **55**, 3934 (1997).
[17] E. Nogueira, Jr., S. Coutinho, F. D. Nobre, and E. M. F. Curado, Short-range ising spin glasses: A critical exponent study, Physica A **257**, 365 (1998).
[18] E. Nogueira, Jr., S. Coutinho, F. D. Nobre, and E. M. F. Curado, Universality in short-range ising spin glasses, Physica A **271**, 125 (1999).
[19] E. M. F. Curado, F. D. Nobre, and S. Coutinho, Ground-state degeneracies of ising spin glasses on diamond hierarchical lattices, Phys. Rev. E **60**, 3761 (1999).
[20] F. D. Nobre, On the universal behavior of two-dimensional ising spin glasses, Physica A **280**, 456 (2000).
[21] B. Drossel, H. Bokil, M. A. Moore, and A. J. Bray, The link overlap and finite size effects for the 3D ising spin glass, Eur. Phys. J. B **13**, 369 (2000).
[22] F. D. Nobre, Phase diagram of the two-dimensional ±J ising spin glass, Phys. Rev. E **64**, 046108 (2001).
[23] F. D. Nobre, The two-dimensional ±J ising spin glass: A model at its lower critical dimension, Physica A **319**, 362 (2003).
[24] O. R. Salmon and F. D. Nobre, Spin-glass attractor on tridimensional hierarchical lattices in the presence of an external magnetic field, Phys. Rev. E **79**, 051122 (2009).
[25] O. R. Salmon, B. T. Agostini, and F. D. Nobre, Ising spin glasses on Wheatstone-bridge hierarchical lattices, Phys. Lett. A **374**, 1631 (2010).
[26] S. T. O. Almeida, E. M. F. Curado, and F. D. Nobre, Chaos and stiffness exponents for short-range Gaussian ising spin glasses, J. Stat. Mech. (2013) P06013.
[27] T. Jörg and H. G. Katzgraber, Evidence for universal scaling in the spin-glass phase, Phys. Rev. Lett. **101**, 197205 (2008).
[28] A. A. Migdal, Phase transitions in gauge and spin-lattice systems, Sov. Phys. JETP **42**, 743 (1976).
[29] L. P. Kadanoff, Notes on Migdal's recursion formulas, Ann. Phys. **100**, 359 (1976).
[30] H. G. Katzgraber, M. Körner, and A. P. Young, Universality in three-dimensional ising spin glasses: A Monte Carlo study, Phys. Rev. B **73**, 224432 (2006).
[31] W. L. McMillan, Domain-wall renormalization-group study of the two-dimensional random ising model, Phys. Rev. B **29**, 4026 (1984).
[32] W. L. McMillan, Domain-wall renormalization-group study of the three-dimensional random ising model, Phys. Rev. B **30**, 476 (1984).
[33] A. J. Bray and M. A. Moore, Lower critical dimension of ising spin glasses: A numerical study, J. Phys. C **17**, L463 (1984).
[34] W. L. McMillan, Domain-wall renormalization-group study of the three-dimensional random ising model at finite temperature, Phys. Rev. B **31**, 340 (1985).
[35] A. K. Hartmann, Scaling of stiffness energy for three-dimensional ±J ising spin glasses, Phys. Rev. E **59**, 84 (1999).
[36] A. K. Hartmann and A. P. Young, Lower critical dimension of ising spin glasses, Phys. Rev. B **64**, 180404 (2001).
[37] S. Boettcher, Stiffness of the Edwards-Anderson model in all dimensions, Phys. Rev. Lett. **95**, 197205 (2005).
[38] A. P. Young and H. G. Katzgraber, Absence of an Almeida-Thouless line in three-dimensional spin glasses, Phys. Rev. Lett. **93**, 207203 (2004).
[39] T. Jörg, H. G. Katzgraber, and F. Krząkała, Behavior of ising spin glasses in a magnetic field, Phys. Rev. Lett. **100**, 197202 (2008).
[40] E. Marinari, G. Parisi, and J. J. Ruiz-Lorenzo, in *Spin Glasses and Random Fields*, edited by A. P. Young (World Scientific, Singapore, 1998), p. 59.
[41] M. Hasenbusch, A. Pelissetto, and E. Vicari, The critical behavior of 3D ising spin glass models: Universality and scaling corrections, J. Stat. Mech. (2008) L02001.
[42] M. Hasenbusch, A. Pelissetto, and E. Vicari, Critical behavior of three-dimensional ising spin glass models, Phys. Rev. B **78**, 214205 (2008).
[43] M. Baity-Jesi *et al.*, Critical parameters of the three-dimensional ising spin glass, Phys. Rev. B **88**, 224416 (2013).
[44] S. T. O. Almeida and F. D. Nobre, Fixed-point distributions of short-range ising spin glasses on hierarchical lattices, Phys. Rev. E **91**, 032138 (2015).
[45] W. A. M. Morgado, S. Coutinho, and E. M. F. Curado, Multifractal magnetization on hierarchical lattices, J. Stat. Phys. **61**, 913 (1990).
[46] A. Rosas and S. Coutinho, Random-field ising model on hierarchical lattices: Thermodynamics and ground-state critical properties, Physica A **335**, 115 (2004).
[47] O. Melchert, AutoScale.py—A program for automatic finite-size scaling analyses: A user's guide, arXiv:0910.5403.
[48] F. Antenucci, A. Crisanti, and L. Leuzzi, Critical study of hierarchical lattice renormalization group in magnetic ordered and quenched disordered systems: Ising and Blume-Emery-Griffiths models, J. Stat. Phys. **155**, 909 (2014).
[49] J. R. L. de Almeida, Perturbation study of the linear renormalization group for spin glasses, J. Phys. A **26**, 193 (1993).
[50] C. Tsallis, On the hierarchical lattices approximation of Bravais lattices: Specific heat and correlation length, J. Phys. C **18**, 6581 (1985).
[51] J. R. Melrose, Hierarchical ensembles: Random fractals, flow fractals and the renormalisation group, J. Phys. A **19**, 2395 (1986).
[52] J. A. Redinz, A. C. N. Magalhães, and E. M. F. Curado, Potts antiferromagnetic model on a family of fractal lattices: Exact results for an unusual phase, Phys. Rev. B **49**, 6689 (1994).
[53] J. A. Redinz and A. C. N. Magalhães, Ising ferromagnet on a fractal family: Thermodynamical functions and scaling laws, Phys. Rev. B **51**, 2930 (1995).
[54] L. da Silva, E. M. F. Curado, S. Coutinho, and W. A. M. Morgado, Criticality and multifractality of the Potts ferromagnetic model on fractal lattices, Phys. Rev. B **53**, 6345 (1996).
[55] J. A. Redinz, Ising ferromagnet in fractal lattices: Analytical verification of the hyperscaling law, J. Phys. A **31**, 6921 (1998).